Micromixing Efficiency of a Novel Sliding-Surface Mixing Device

Jean-Marc Rousseaux, Laurent Falk, Hervé Muhr, and Edouard Plasari
Laboratoire des Sciences du Génie Chimique CNRS—Ecole Nationale Supérieure des Industries Chimiques INPL, 1, rue grandville BP 451, 54 001 Nancy Cedex, France

A new mixing device, suitable to achieve the mixing of reactants undergoing fast chemical reactions, is studied. In the sliding-surface mixing device, the chemical reagents are introduced in a confined mixing zone (CMZ), in which high shearing stresses are created in a very small volume to realize rapid micromixing. A system of parallel competing test reactions was used to characterize the micromixing level in the CMZ as a function of feed flow rate, rotation speed, feed pipe position, and a geometric parameter characterizing the CMZ. The influence of these parameters on micromixing efficiency was studied, and a hydrodynamic model was developed. This model successfully predicts micromixing times that were measured at two different flow regimes, two feed points, four recirculation flow rates, three geometric configurations, and various stirrer speeds.

Introduction

The control of the size distribution of particles produced by precipitation can have important effects on ease of manufacture and product quality in the fine-chemical and pharmaceutical industries. In industrial practice, the precipitation operation typically consists of mixing two liquid streams in order to create supersaturation, which then induces nucleation, particle growth, aggregation, and agglomeration.

It is well known that the way in which reagents are mixed can have a large influence on the product distribution of a chemical reaction. Micromixing, or mixing at the fine scales, has been shown to be primarily responsible for this influence, mainly affecting crystal size distribution (Pohorecki and Baldyga, 1988; Marcant and David, 1991; Franke and Mersmann, 1995). The reason for this is that precipitation kinetics are controlled by supersaturation, that is, concentration field, with reaction times that are generally smaller than the characteristic time of micromixing.

Downstream processing of a precipitate requires filtration of the product, frequently followed by washing and drying. For each of these operations, poor control of the particle-size distribution may generate a large amount of fines, which could lead to difficult processing and cost increases. Furthermore, yield and selectivity may be reduced, which for high-value products such as pharmaceuticals may be of great importance.

For these reasons, new technologies are developed to perform precipitation processes capable of producing particles with controlled properties.

Several mixers, characterized by a confined mixing zone (CMZ) and suitable for very effective micromixing, have been studied, including, the centrifugal pump (Bolzern and Bourne, 1985), the pipeline (Bourne and Tovstiga, 1988; Li and Toor, 1986) and rotor-stator mixers of various sizes (Bourne and Garcia-Rosas, 1986; Bourne and Studer, 1992). Otherwise, as far as a rotating disk used as an agitator is concerned, the efficiency of a high-speed spinning disk was studied and compared to a Rushton turbine in a tank of standard geometry by Deglon et al. (1998). More generally, Schlichting (1968) studied the flow in the neighborhood of a rotating disk, which is of great practical importance, particularly in connection with rotary machines (lubrication).

In this work, a stirred tank equipped with a rotating disk has been designed to produce particles with controlled properties. The rotating disk is used to create a CMZ in which high shearing stresses can be achieved in order to realize rapid micromixing of reagent feed streams in a very small, controlled volume. In addition, this mixing device separates the reactor into two mixing zones: one CMZ and one moderately mixed zone where particles can undergo an aging step, which

Correspondence concerning this article should be addressed to J.-M. Rousseaux.

may be of paramount importance for some precipitation processes.

The aim of this work is to study the influence of some operating parameters on the micromixing time in the CMZ of this new sliding-surface mixing device. For this purpose, a chemical reaction method (based on the Dushman's reaction and developed by Villermaux et al., 1994) is presented and used to measure the micromixing level induced by the spinning disk at the feed point location. Micromixing time can then be deduced from the experiments using a micromixing model, namely the incorporation model. In order to correlate micromixing times with the operating parameters, a model is developed from hydrodynamic and dimensional analysis considerations. This model enables one to obtain a fairly good estimation of the micromixing times, which is vital for the optimization and scale-up of the reactor.

Determination of Micromixing Time

Characterization of micromixing

Many physical and chemical methods, some easier to handle than others, have been developed to characterize micromixing efficiency. The method used in the present work is based on a competitive parallel reaction system, which has been studied extensively by Fournier (1994), Fournier et al. (1996), and Guichardon (1996):

$$H_2BO_3^- + H^+ \rightarrow H_3BO_3 \qquad \text{quasi instantaneous} \qquad \text{(i)}$$

$$5I^- + IO_3^- + 6H^+ \rightarrow 3I_2 + 3H_2O \qquad \text{very fast.} \qquad \text{(ii)}$$

The redox reaction (ii) is very fast, in the same range of the micromixing process, but is much slower than the neutralization reaction (i). The iodine formed can further react with iodide ions I^- to yield I_3^- ions according to the quasi-instantaneous equilibrium:

$$I_2 + I^- \Leftrightarrow I_3^-. \qquad \text{(iii)}$$

The concentration of I_3^- ions can easily be measured by a spectrophotometer at 353 nm according to the Beer-Lambert's law (Guichardon, 1996):

$$(I_3^-) = \frac{OD}{\epsilon_{353} L} \qquad (1)$$

where L is the quartz cell thickness, OD the optical density, and ϵ_{353} the molar extinction coefficient of triiodide ions at 353 nm.

The test procedure consists of adding, in stoichiometric deficiency, a small quantity of sulfuric acid to a mixture of iodate, iodide, and borate ions. Under perfect mixing conditions, the injected acid is instantaneously dispersed in the reactive medium and consumed by borates according to neutralization reaction (i), which is infinitely faster than reaction (ii). On the other hand, when the characteristic dissipation time of the acid aggregates t_m (micromixing time) is in the same range or larger than the characteristic reaction time of the redox reaction (reaction ii), these aggregates involve a local overconcentration of acid which, after complete consumption of local $H_2BO_3^-$ ions, can react with the surrounding iodide and iodate ions to produce iodine. The selectivity of iodine is thus a measure of the fluid segregation state.

Determination of the segregation index

The segregation index is defined as the relative amount of acid that is consumed to yield iodine. We know that the values of the segregation index lie between 0 and 1:

$$\text{for perfect micromixing (PM)} \qquad X_S = 0 \qquad (2)$$

$$\text{for total segregation (TS)} \qquad X_S = 1 \qquad (3)$$

$$\text{for partial segregation} \qquad X_S = \frac{Y}{Y_{TS}}, \qquad (4)$$

where Y is the iodine yield, and Y_{TS} the yield under TS conditions. The expressions of Y and Y_{TS} are reported by Fournier et al. (1996), and are expressed as follows:

$$Y = \frac{2(n_{I_2} + n_{I_3^-})}{n^0_{H^+}} = \frac{2V_{\text{reactor}}\left[(I_2) + (I_3^-)\right]}{V_{\text{injection}}(H^+)_0} \qquad (5)$$

$$Y_{TS} = \frac{6n^0_{IO_3^-}}{6n^0_{IO_3^-} + n^0_{H_2BO_3^-}} = \frac{6(IO_3^-)_0}{6(IO_3^-)_0 + (H_2BO_3^-)_0}. \qquad (6)$$

In order to calculate $X_S = (Y/Y_{TS})$, the concentration of the iodide ions (I^-) has to be determined. A material balance and the equilibrium constant of equilibrium reaction (iii), K_{iii}, enables us to write (Palmer and Lietzke, 1982)

$$(I^-) = (I^-)_0 - \frac{5}{3}\left[(I_2) + (I_3^-)\right] - (I_3^-) \qquad (7)$$

$$K_{iii} = \frac{(I_3^-)}{(I_2)(I^-)}. \qquad (8)$$

By combining these two equations, a second-order equation is obtained that allows the determination of the iodine concentration (I_2):

$$-\frac{5}{3}(I_2)^2 + \left[(I^-)_0 - \frac{8}{3}(I_3^-)\right](I_2) - \frac{(I_3^-)}{K_{iii}} = 0. \qquad (9)$$

The equilibrium constant K_{iii} is given as a function of temperature T (K) (Guichardon, 1996):

$$\log_{10} K_{iii} = \frac{555}{T} + 7.355 - 2.575\log_{10}(T) \quad \left(K_{iii} \text{ in } L \cdot mol^{-1}\right). \qquad (10)$$

Assuming that the real fluid can be separated in one perfectly micromixed volume (V_{PM}) and one totally segregated (V_{TS}) volume, the following equation is written:

$$(V_{PM} + V_{TS})X_S = V_{PM}(X_S)_{PM} + V_{TS}(X_S)_{TS}.$$

Hence

$$(V_{PM} + V_{TS})X_S = V_{TS}. \qquad (11)$$

From this equation, a micromixing parameter, the micromixedness ratio α, is introduced, which is interpreted as the ratio of the perfectly micromixed volume fraction to the segregated volume fraction in the mixing plume:

$$\alpha = \frac{V_{PM}}{V_{TS}} = \frac{1 - X_S}{X_S}. \tag{12}$$

The reagent concentrations used in this work are the following:

$$(I_2)_{\text{potentially formed}} = 3(IO_3^-)_0 = 3/5(I^-)_0 = 7 \cdot 10^{-3} \text{ mol} \cdot \text{L}^{-1}$$
$$(H_3BO_3)_0 = 0.1818 \text{ mol} \cdot \text{L}^{-1}$$
$$(NaOH)_0 = 0.0909 \text{ mol} \cdot \text{L}^{-1}$$
$$(H_2SO_4)_0 = 0.5 \text{ mol} \cdot \text{L}^{-1}.$$

For these reagent concentrations, the resolution of Eqs. 1, 4–6, 9, 10, and 12 enables the correlation of the micromixedness ratio α to the optical density (OD):

$$\alpha = \frac{1 - X_s}{X_s} = 5.34(\text{OD})^{-1.24} \tag{13}$$

Calculation of micromixing time values

The incorporation model, derived from earlier works by Villermaux (1990), and clearly described by Fournier et al. (1996), is used to determine the micromixing time.

The incorporation model supposes that the fresh acid is divided into aggregates that are progressively invaded by the surrounding fluid, which contains iodide, iodate, and borate ions. Reactions (i)–(iii) occur in the growing acid aggregates, where mixing is assumed to be achieved. The growth law of the acid aggregates is a function of a characteristic incorporation time t_m, assumed to be the micromixing time.

The incorporation process is due to the formation of small-scale vortices in the fluid. The vortex of incorporated volume V grows at a rate of V/t_m by inflow from the surroundings:

$$\frac{dV}{dt} = \frac{V}{t_m}. \tag{14}$$

Because diffusion within the deforming engulfed structure is usually much faster than incorporation, the concentration of any substance i inside the deforming engulfed structure is uniform and is represented by c_i. The corresponding concentration in the immediate surroundings of the growing vortex is $\langle c_i \rangle$. For a semi-batch reactor operating with a low feed rate, adequate time is available for the flow and mixing to homogenize in the vessel, so that $\langle c_i \rangle$ is the average concentration of substance i in the vessel. Thus, any inhomogeneity exists only in the reaction zone and is due to inadequate micromixing. Each aggregate can be considered individually with no interaction with the other aggregates. As the volume of acid injected in the tank is low compared to the whole volume of the tank, $\langle c_i \rangle$ can be considered constant. The mass-balance equation for one aggregate is then representative of all the aggregates. Thus, the mass balance of substance i in the reaction zone is

$$\frac{d(Vc_i)}{dt} = \frac{dV}{dt}\langle c_i \rangle + r_i V, \tag{15}$$

where r_i is the rate of formation of i by reaction (mol·m^{-3}·s^{-1}), as given by chemical kinetics.

Rearrangement of Eq. 15 leads to

$$\frac{d(c_i)}{dt} = \frac{1}{V}\frac{dV}{dt}(\langle c_i \rangle - c_i) + r_i. \tag{16}$$

This mass balance is valid for turbulent micromixing (Baldyga and Bourne, 1990), as well as for laminar micromixing (Baldyga et al., 1998). Combining Eqs. 14 and 16, one obtains

$$\frac{dc_i}{dt} = \frac{\langle c_i \rangle - c_i}{t_m} + r_i. \tag{17}$$

Numerical integration of Eq. 17 gives the concentration of all substances in the growing reaction zone as a function of time. Integration stops when the limiting reagent has been consumed. The final mean concentrations of all substances are then found and this allows calculation of the corresponding value of α. Using this procedure, the theoretical value of α for each given micromixing time value and for the initial reagent concentrations used in this work is calculated. The micromixing time as a function of calculated micromixedness ratio is represented in Figure 1. In order to facilitate the numerical treatment of the experimental data, the results of Figure 1 are expressed in the form of three equations obtained by regression analysis:

$$2 < \alpha < 5 \quad t_m = 0.73\alpha^{-2.26} \tag{18}$$
$$5 < \alpha < 7 \quad t_m = 0.82\alpha^{-2.30} \tag{19}$$
$$7 < \alpha < 20 \quad t_m = 0.158\alpha^{-1.45}. \tag{20}$$

Equations 18, 19, and 20 are quite useful for determining the micromixing time in other chemical reactors characterized by a segregation index α of values between 2 and 20.

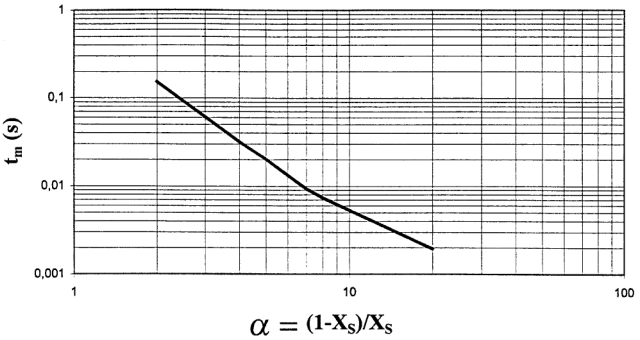

Figure 1. Micromixing time t_m vs. micromixedness ratio $\alpha = (1 - X_S)/X_S$.

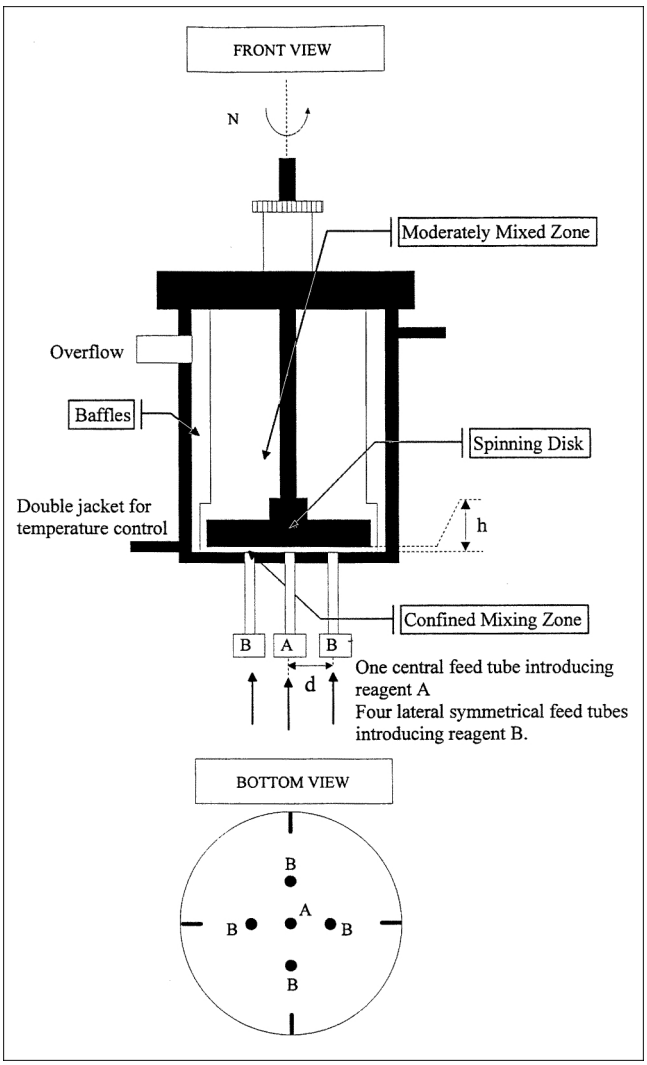

Figure 2. Front and bottom views of the sliding-surface mixing device investigated.

Experimental Studies

Presentation of the sliding-surface mixing device

The sliding-surface mixing device (see Figure 2 and Table 1) is composed of a 2.5-liter tank of inner diameter 0.15 m equipped with a rotating disk whose diameter is equal to 80% of the inner diameter of the tank. This device separates the reactor into two mixing zones. The first, the confined mixing zone (CMZ), is situated between the sliding disk and the bottom of the reactor, where the reactants are introduced. One central feed tube (tube diameter 2 mm) introduces reagent *A*, and four lateral symmetrical feed tubes (tube diameter 2 mm), all situated at equal distance *d* from the central feed tube, introduce reagent *B*. The gap *h* between the sliding disk and the bottom of the reactor can be varied. In this way, it is possible to change the mean residence time inside the CMZ (see Table 2). The dual purpose of creating such a confined mixing zone inside the stirred-tank reactor is to (1) cause a highly reproducible supersaturation of the reagents in a perfectly defined zone, and (2) to create a very highly localized shear stress at the very point where the reagents are fed, so as to achieve rapid micromixing of the reagent feed streams.

Table 1. Dimensions and Characteristics of the Sliding-Surface Mixing Device

Total tank volume	2.5 L
Diameter of the tank	150 mm
Height of the tank	150 mm
Diameter of the spinning disk	120 mm
Thickness of the spinning disk	10 mm
Gap between spinning disk and bottom of reactor	1 mm to 3.5 mm
Width of the four baffles	15 mm
Diameter of feed pipes	2 mm
Spacing between the central feed pipe and the lateral symmetrical feed pipes	17.5 or 40.0 mm
Rotating disk speed	up to 50 s^{-1}
Recirculation flow rate	up to 500 $mL \cdot min^{-1}$

The second zone, the moderately mixed zone (MMZ), is situated above the sliding disk, where, by controlling the residence time and the temperature inside the reactor, particles can undergo an aging step.

Experimental setup and experimental conditions investigated

The spinning disk is driven by an electric motor: a D71SK Brook Hansen operated by a Falcon Drives VPM SLm frequency variator. This motor has a power output of 0.55 kW, a maximum rotation speed of 3,000 rpm, and a torque of 1.86 Nm. The rotation speed has a frequency stability of $\pm 0.05\%$. The iodide–iodate–borate solution is recirculated from the bulk of the reactor to the middle of the confined mixing zone by a Masterflex peristaltic pump. The recirculation flow rate is determined by a rotameter. A second Masterflex peristaltic pump makes it possible to carefully introduce a well-defined volume of sulfuric acid at the point in the reactor where micromixing should be characterized. A Jobin Yvon Hitachi Double Beam Model 100-60 spectrophotometer is used to measure the concentration of I_3^- ions thanks to two Hellma Type 100 QS 10-mm dishes. Finally, a syringe to squirt a sample from the bulk of the reactor is used, and the injection time is determined with a chronometer.

The experimental setup is shown in Figure 3.

The *process parameters* studied are the mixing speed (N), and the recirculation flow rate (Q):

- N (s^{-1}): 9; 12; 16; 20; 30; 40; 50
- Q ($mL \cdot min^{-1}$): 60; 120; 240; 480.

The *geometric parameters* (see Figure 2) of the sliding-surface mixing device are the height h between the sliding disk and the bottom of the reactor, and the distance d between the central feed pipe of the recirculated reactive solu-

Table 2. Mean Residence Time Inside the CMZ as a Function of Flow Rate and Gap Height

Q ($mL \cdot min^{-1}$)	$h = 1.5$ mm (s)	$h = 2$ mm (s)	$h = 2.5$ mm (s)
60	17.0	22.6	28.3
120	8.5	11.3	14.1
240	4.2	5.7	7.1
480	2.1	2.8	3.5

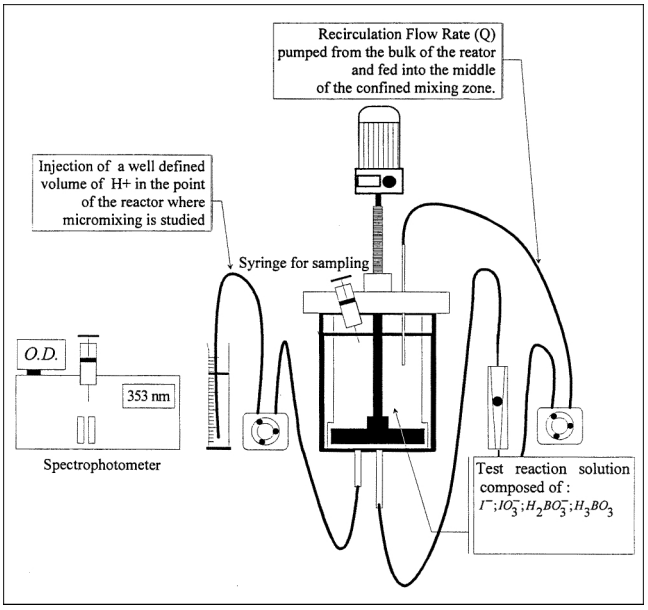

Figure 3. Experimental setup.

tion and the feed pipe of H^+ ions arriving at the point in the confined mixing zone where the micromixing time should be determined:

- d (mm): 17.5; 40.0
- h (mm): 1.5; 2; 2.5.

Experimental procedure

The first (acid) solution is prepared with a commercial concentrated solution ($36N$) of sulfuric acid. The preparation of the second solution needs some precautions. KI and KIO_3 powders are first dissolved in separate vessels. H_3BO_3 and NaOH are then mixed to obtain the buffer solution, to which the KI and KIO_3 solutions and water are added. This sequence of the mixing operation must be carefully followed. In this way, iodide and iodate ions coexist in a basic solution that prevents iodine (I_2) formation.

Our procedure for characterizing micromixing is perfectly adapted for standard stirred vessels (for which the micromixedness ratio α is classically between 2 and 20). For a stirred tank of L liters, $4\cdot10^{-3}\times L$ liters of sulfuric acid ($1N = 0.5\ \text{mol}\cdot\text{L}^{-1}$) have to be injected into the mixture containing the iodide, iodate (stoichiometric mixture), and borate ions with the following concentrations (Guichardon, 1996):

$$(I_2)_{\text{potentially formed}} = 3(IO_3^-)_0 = 3/5(I^-)_0 = 7\cdot10^{-3}\ \text{mol}\cdot\text{L}^{-1}$$

$$(H_3BO_3)_0 = 0.1818\ \text{mol}\cdot\text{L}^{-1}$$

$$(NaOH)_0 = 0.0909\ \text{mol}\cdot\text{L}^{-1}.$$

As a strong base, sodium hydroxide totally reacts with orthoboric acid to form an equimolar mixture $H_2BO_3^-/H_3BO_3$. The pH of the buffer is then equal to $pK_{a1} = 9.14$, which corresponds to the first acidity of orthoboric acid. As a consequence, once fresh iodide–iodate–borate solution is prepared, we have: $(H_3BO_3) = (H_2BO_3^-) = 0.0909\ \text{mol}\cdot\text{L}^{-1}$.

In this work, 10 mL of $1N$ sulfuric acid are injected in the reactor at the very point of the CMZ where micromixing is investigated (see Figure 4). As the four lateral feed tubes are symmetrical, the acid is injected in only one feed tube, the other three being blocked. The sulfuric acid reacts with the iodide, iodate, and borate solution, which is recirculated from the bulk of the reactor into the central feed tube of the CMZ with a given flow rate.

In order to characterize micromixing without macromixing influence, the acid feed rate must be as low as possible. Indeed, it is well known that the acid feed time (or the acid feed flow rate, since a constant quantity of acid is injected) has an influence on the segregation index (Bourne and Thoma, 1991; Baldyga and Bourne, 1992). It decreases when the feed time increases to reach a constant value. The critical feed time t_c is defined as the minimum time beyond which the segregation index value remains constant. This phenomenon translates the fact that for feed times higher than t_c only micromixing determines the value of X_S, whereas for feed times smaller than t_c, the segregation index is controlled by both macro- and micromixing. Actually, this injection time has to be redetermined for each new set of operating conditions.

Two minutes after the acid injection, a sample of the solution is taken, whatever the position in the tank, to determine the OD of I_3^- ions by spectrophotometry at 353 nm. Thanks to the good stability of I_3^-, the measurements can be carried out with a good accuracy up to 10 min after the acid injection.

In a first version of the sliding-surface mixing device, the diameter of the injection tubes was 4 mm. In this case, under the same operating conditions, aleatory variations of the micromixing time values were obtained due to back-mixing fluctuations in the tube. The same phenomenon has been observed by Baldyga et al. (1993), while the back-mixing of reagents in the feed pipe of stirred reactors has been photographed by Bourne et al. (1981). These authors recommend the use of small tube diameters in order to eliminate the influence of back-mixing on the determination of the micromixing time. In the case of the sliding-surface mixing device,

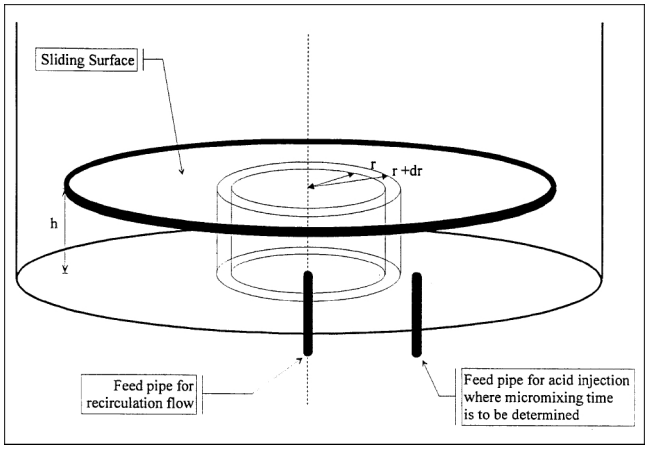

Figure 4. Confined mixing zone.

reproducible micromixing time values are obtained when tubes of 4-mm diameter are replaced by tubes of 2-mm diameter.

Three to five experiments are carried out for each group of fixed experimental parameter values, and each representative micromixing time value is the mean of the experimental values found. In any case, a statistical treatment of the experimental data gives a relative error of the micromixing time not exceeding 15%.

Theoretical Expressions of the Micromixing Time Inside the CMZ

For turbulent flows and for Sc < 4,000, Baldyga and Bourne (1990) proposed

$$t_m = 17.2\sqrt{\frac{\nu}{\epsilon}}, \tag{21}$$

where ϵ is the rate of energy dissipation and ν the kinematic viscosity.

According to Villermaux (1986), even in the absence of turbulence, mixing occurs under the influence of the convective velocity field. Fluid aggregates are stretched out and folded up and the mixture finally exhibits a lamellar or striated structure characterized by a striation thickness δ. In Newtonian liquids, a lower bound for the stretching time is found to be (Villermaux, 1986)

$$t_\delta = \sqrt{\frac{2\nu}{\epsilon}}. \tag{22}$$

Hence, the micromixing time in laminar flow is related to the energy dissipation rate by an effect similar to the turbulent flow. Consequently, for both the laminar and turbulent flow regimes, we have

$$t_m \propto \sqrt{\frac{\nu}{\epsilon}}. \tag{23}$$

According to Eq. 23, we can see that micromixing time is related to the rate of energy dissipation ϵ. Let us estimate the contributions of the spinning disk and the recirculation flow to the local specific power input. Figure 4 shows a geometric scheme of the CMZ that can be used to obtain mathematical expressions of the energy dissipation rate.

Contribution of the spinning disk to the local specific power input

Newton's law, applied to a ring of radius r and width dr on the spinning disk, can be written as

$$dF(r) = \tau(r)dS(r) \quad \text{with} \quad dS(r) = 2\pi r \times dr, \tag{24}$$

where $\tau(r)$ is the shearing stress at a distance r from the axis, and $dS(r)$ is the surface of the annular element with width dr.

The tangential velocity at a distance r from the axis is equal to

$$v(r) = 2\pi Nr. \tag{25}$$

Thus, the elementary power induced by the rotation of the disk ring of radius r and width dr can be written as

$$dP_1 = v(r)dF(r). \tag{26}$$

The local specific power input due to the rotation of the disk at an injection point situated at a radius r from the center of the CMZ can be written as

$$\epsilon_1(r) = \frac{dP_1(r)}{dm} = \frac{2\pi rN}{\rho h}\tau(r), \tag{27}$$

where $dm = \rho dV$ with $dV = h \times 2\pi r \times dr$.

The expression of the shearing stress depends upon the flow regime, so two cases have to be distinguished: laminar flow and turbulent flow.

Laminar Flow. The variation of the tangential velocity across the gap is linear in the manner of Couette flow. Hence, the shearing stress at a distance r from the axis is equal to

$$\tau(r) = \mu\frac{2\pi Nr}{h}. \tag{28}$$

Substituting Eq. 26 into Eq. 25, the expression of the specific power input due to the rotation speed of the spinning disk at an injection point situated at a radius r from the center of the CMZ becomes

$$\epsilon_1(r) = \frac{\mu}{\rho}\frac{(2\pi r)^2N^2}{h^2}. \tag{29}$$

Knowing that $\nu = \mu/\rho$, we have

$$\epsilon_1(r) = \nu\frac{(2\pi r)^2N^2}{h^2}. \tag{30}$$

Turbulent Flow. According to Schlichting (1968, chap. XXI), the shearing stress in this case is proportional to the following parameters expressed with the aid of Eq. 31:

$$\tau(r) \propto \rho(2\pi Nr)^{7/4}\left(\frac{\nu}{h}\right)^{1/4}. \tag{31}$$

Finally, substituting Eq. 31 into Eq. 27, the expression of the specific power input due to the rotation speed of the spinning disk at an injection point situated at a radius r from the center of the CMZ is expressed as

$$\epsilon_1(r) \propto (rN)^{11/4}\frac{\nu^{1/4}}{h^{1/4}}. \tag{32}$$

Contribution of the recirculation flow to the local specific power input

The local specific power input due to the recirculation flow can be evaluated thanks to the pressure drop undergone by the fluid when the fluid flows radially through the CMZ.

The mean radial velocity component of the fluid flowing

radially through the CMZ at radius r can be written as

$$\bar{u}(r) = \frac{Q}{2\pi rh}. \tag{33}$$

To determine the pressure drop, it is convenient to work with the Moody friction factor, which is a dimensionless parameter defined as (Incropera and DeWitt, 1996)

$$-\frac{dp}{dr} = f\frac{1}{d_H}\frac{\rho\bar{u}^2}{2}, \tag{34}$$

where f is the friction factor and d_H the hydraulic diameter defined as

$$d_H = \frac{4\times 2\pi rh}{2\times 2\pi r} = 2h.$$

The elementary pressure drop of a fluid flowing laterally from radius r to radius $r + dr$ inside the CMZ can be written as

$$-dp = f\frac{\rho\bar{u}^2}{2d_H}dr. \tag{35}$$

Hence, the elementary power dissipation is

$$dP_2 = Q(-dp) = f\frac{Q\rho\bar{u}^2}{2d_H}dr. \tag{36}$$

As in Eq. 27, the local specific power input due to the recirculation flow rate at an injection point situated at a radius r from the center of the CMZ can be written as:

$$\epsilon_2(r) = \frac{dP_2(r)}{dm}, \tag{37}$$

where $dm = \rho dV$ with $dV = h\times 2\pi r\times dr$.

Finally, from Eqs. 33, 36, and 37, the expression of the specific power dissipation due to the recirculation flow rate becomes

$$\epsilon_2(r) = \frac{f}{32\pi^3}\frac{Q^3}{h^4r^3}. \tag{38}$$

The expression of the friction factor depends upon the flow regime, so two cases have to be distinguished: laminar flow and turbulent flow.

The expressions of the friction factor are:
For laminar flow (Incropera and DeWitt, 1996):

$$f = \frac{96}{Re_{D_H}} = 96\frac{\nu}{2\bar{u}(r)h}. \tag{39}$$

For turbulent flow (Schlichting, 1968):

$$f \propto Re^{-1/5} \propto \left[\frac{\nu}{\bar{u}(r)h}\right]^{1/5}. \tag{40}$$

Knowing that $Q = 2\pi rh\bar{u}(r)$, Eqs. 39 and 40 give
For laminar flow:

$$f = 96\pi\frac{r\nu}{Q}. \tag{41}$$

For turbulent flow:

$$f \propto \left[\frac{r\nu}{Q}\right]^{1/5}. \tag{42}$$

Hence, the two following equations are obtained:
For laminar flow:

$$\epsilon_2(r) = \frac{3}{\pi^2}\frac{Q^2\nu}{h^4r^2}. \tag{43}$$

For turbulent flow:

$$\epsilon_2(r) \propto \frac{Q^{14/5}\nu^{1/5}}{h^4r^{14/5}}. \tag{44}$$

Expressions of the total specific power dissipation

The total specific energy dissipation rate comprises a contribution ϵ_1 from mechanical agitation and a contribution ϵ_2 from the friction associated with the radial flow of the entering fluid. From experience, it seems that ϵ_1 and ϵ_2 contribute to micromixing with different efficiencies, η_1 and η_2. According to Villermaux (1986), their contributions to the total specific energy dissipation rate are linearly additive and can be written as follows:

$$\epsilon = \eta_1\epsilon_1 + \eta_2\epsilon_2.$$

This expression has been successfully used by Plasari et al. (1978) and Klein et al. (1980) to model micromixing phenomena in continuous-stirred reactors. Hence, the total specific power dissipation can be written as follows:
For laminar flow:

$$\epsilon_L(r) = A'_L\left[\frac{rN}{h}\right]^2\nu + B'_L\left[\frac{Q}{r}\right]^2\frac{\nu}{h^4}. \tag{45}$$

For turbulent flow:

$$\epsilon_T(r) = A'_T(rN)^{11/4}\frac{\nu^{1/4}}{h^{5/4}} + B'_T\left[\frac{Q}{r}\right]^{14/5}\frac{\nu^{1/5}}{h^4}, \tag{46}$$

where A'_L, B'_L, A'_T, and B'_T in Eqs. 45 and 46 are intermediary proportionality constants.

Expression of the model equations for the micromixing time

In our case, $Sc < 4{,}000$, so the model equations for the micromixing time can be obtained from Eqs. 23 and Eqs. 45 and 46:

Laminar flow:

$$t_m = \frac{1}{\sqrt{A_L\left[\frac{rN}{h}\right]^2 + B_L\left[\frac{Q}{r}\right]^2 \frac{1}{h^4}}}. \quad (47)$$

Turbulent flow:

$$t_m = \frac{1}{\sqrt{A_T(rN)^{11/4}\frac{\nu^{-3/4}}{h^{5/4}} + B_T\left[\frac{Q}{r}\right]^{-14.5}\frac{\nu^{-4/5}}{h^4}}}. \quad (48)$$

In Eqs. 47 and 48, A_L, B_L, A_T, and B_T are constants to be determined from the experimental results.

Determination of the flow regime

The rotational Reynolds number (at a distance r from the axis) of a rotating disk is defined as

$$Re(r) = \frac{r^2\omega}{\nu} = \frac{r^2 2\pi N}{\nu}. \quad (49)$$

According to Schlichting (1968, chap. XXI), two flow regimes have to be considered for the flow around a disk rotating in a housing:

- For $\mathrm{Re}(r) < 10^5$, the flow is laminar.
- For $\mathrm{Re}(r) > 3\cdot 10^5$, the flow becomes turbulent.

It appears from Table 3 that the flow regime is always laminar (even when $N = 50\ \mathrm{s}^{-1}$) at a distance of 17.5 mm from the center, while at a distance of 40.0 mm from the center, the flow regime is turbulent for values of a rotation speed higher than $30\ \mathrm{s}^{-1}$.

Results and Discussion

According to Eqs. 47 and 48, in the case of laminar flow, the micromixing time is independent of the kinematic viscosity of the reagents, while, in the case of turbulent flow, the micromixing time depends on this parameter.

In all our experiments carried out at 20°C, the kinematic viscosity of the aqueous solutions is equal to $\nu = 10^{-6}\ \mathrm{m^2\cdot s^{-1}}$, so the effect of viscosity has not been studied. For this reason, for aqueous solutions, for which $\nu = 10^{-6}\ \mathrm{m^2\cdot s^{-1}}$, Eq. 48 can be written as follows:

Table 3. Rotational Re No. Inside CMZ as a Function of the Distance from the Center of CMZ and of the Rotation Speed of the Spinning Disk

	$Re\times 10^{-4}$	
$N\ (\mathrm{s}^{-1})$	$r = 17.5$ mm	$r = 40.0$ mm
9	1.73	9.05
12	2.31	12.1
16	3.08	16.1
20	3.85	20.1
30	5.77	30.2
40	7.70	40.2
50	9.62	50.3

$$t_m = \frac{1}{\sqrt{A_T^{aq}(rN)^{11/4}\frac{1}{h^{5/4}} + B_T^{aq}\left[\frac{Q}{r}\right]^{14/5}\frac{1}{h^4}}}. \quad (50)$$

Fitting parameters A_L and B_L to laminar flow (see Eq. 47), and A_T^{aq} and B_T^{aq} to turbulent flow (see Eq. 50) with experimental results gives:

Laminar flow regime: $A_L = 0.0090\ \mathrm{s}^{-4}$ and $B_L = 0.065\ \mathrm{s}^{-4}$.

Turbulent flow regime: $A_T^{aq} = 0.37\ \mathrm{m}^{-3/2}\cdot\mathrm{s}^{-11/2}$ and $B_T^{aq} = 490\ \mathrm{m}^{-8/5}\cdot\mathrm{s}^{-5}$.

Equations 47 and 50 can be generalized as follows:

$$t_m = \frac{1}{\sqrt{\Phi}}, \quad (51)$$

where

For $Re(r) < 10^5$, the flow is laminar and

$$\Phi = 0.0090\left[\frac{rN}{h}\right]^2 + 0.065\left[\frac{Q}{r}\right]^2\frac{1}{h^4}. \quad (52)$$

For $Re(r) > 2.10^5$, the flow is turbulent and

$$\Phi = 0.37(rN)^{11/4}\frac{1}{h^{5/4}} + 490\left[\frac{Q}{r}\right]^{14/5}\frac{1}{h^4}. \quad (53)$$

Equations 51 and 52 are derived using the local energy dissipation rate at the injection point. Thus, it is indirectly assumed that the width of the micromixing zone is small vis-à-vis the distance of the injection point from the axis. Now it is possible to prove this assumption. As a first approximation, when the micromixing zone is not large, its width Δr can be estimated according to

$$\Delta r \approx \bar{u}(r)t_m = \frac{Q}{2\pi rh\sqrt{\Phi}}. \quad (54)$$

Substituting Eqs. 52 and 53 into Eq. 54 gives:

Laminar flow:

$$\Delta r \approx \frac{1}{2\pi}\left[0.0090\left(\frac{r^2N}{Q}\right)^2 + 0.065\frac{1}{h^2}\right]^{-1/2}. \quad (55)$$

Turbulent flow:

$$\Delta r \approx \frac{1}{2\pi}\left[0.37\frac{r^{19/4}N^{11/4}h^{3/4}}{Q^2} + 490\left(\frac{Q}{r}\right)^{4/5}\frac{1}{h^2}\right]^{-1/2}. \quad (56)$$

In laminar flow, the largest micromixing zone corresponds to the operating conditions: $r = 17.5$ mm; $N = 9\ \mathrm{s}^{-1}$; $h = 2.5$ mm; and $Q = 480\ \mathrm{mL\cdot min^{-1}}$. Substitution of these values into Eq. 55 yields $\Delta r = 1.5$ mm. Similarly, in the case of turbulent flow, the largest micromixing zone width corresponds to the operating conditions: $r = 40.0$ mm; $N = 16\ \mathrm{s}^{-1}$; $h = 2.5$ mm; and $Q = 480\ \mathrm{mL\cdot min^{-1}}$. With these values, Eq. 56 gives:

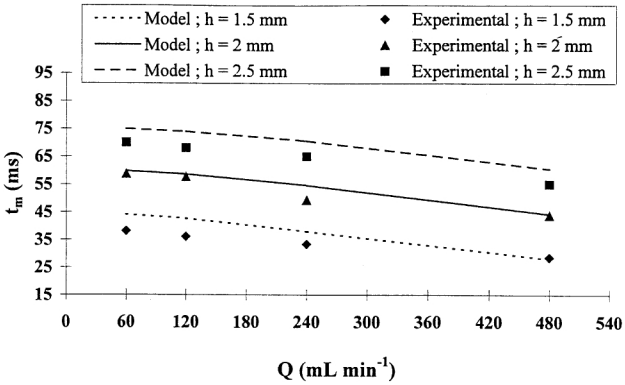

Figure 5. Measured and predicted micromixing times for various disk heights (for $N = 9$ s^{-1} and $r = 40.0$ mm).

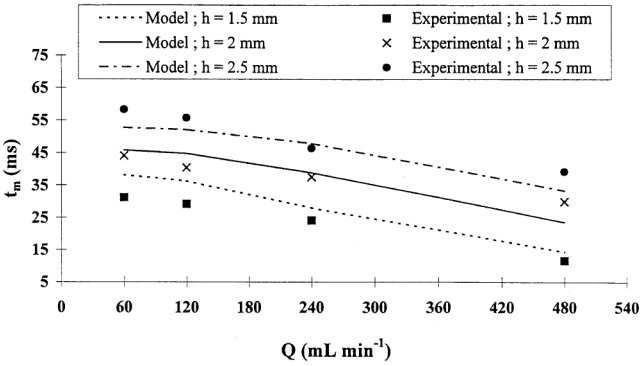

Figure 7. Measured and predicted micromixing times for various disk heights (for $N = 20$ s^{-1} and $r = 40.0$ mm).

$\Delta r = 0.5$ mm. These results prove that the injected substances react in a mixing region of almost constant energy dissipation rate. Our decision to use the local energy dissipation rate to calculate the micromixing times is thus justified.

The experimental results are presented in Figures 5 to 11 as a function of the four operating parameters investigated: N, Q, h, and d, and the experimental values are compared to Eqs. 51, 52, and 53.

Figures 5 to 7 show predicted and measured micromixing times for $d = 40.0$ mm, for three disk heights, and for three rotation speeds. It is clear that the smaller the disk height, the smaller the micromixing time and, similarly, the higher the rotating speed, the smaller the micromixing time. The model curves in Figures 5 and 6 are plotted using the equations for laminar flow (Eqs. 51 and 52), while the model curves of Figure 7 are plotted using the equations for turbulent flow (Eqs. 51 and 53).

The results of Figures 6 and 7 are very interesting because they are located in the interval of the Reynolds number values where the transition from laminar to turbulent flow regime takes place (see Table 3). In this zone, we have seen that the prediction of the experimental results given by Eq. 51 depends on the choice between Eqs. 52 and 53. The experimental results of Figure 6 ($Re = 1.2 \cdot 10^5$) are well predicted by Eq. 52 and correspond to the laminar flow regime, while the experimental results of Figure 7 ($Re = 2 \cdot 10^5$) are well fitted by Eq. 52 and correspond to the turbulent flow regime. As cited earlier, from the dependence of the friction factor vs. the Reynolds number in the case of a disk rotating in a housing (without radial flow), Schlichting (1968) concluded that for $Re < 10^5$ the flow is laminar and for $Re > 3 \cdot 10^5$ the flow is turbulent. Our results show that in the case of micromixing time calculations, these critical values of the Reynolds number remain approximately the same. In addition, it can be concluded that the radial flow existing in our case doesn't influence the interval of the transition of the flow regime.

Figures 8 and 9 refer to the experiments carried out at high rotation speeds (that is, $N = 30$, 40 and 50 s^{-1}) at the feed point situated at $d = 40.0$ mm from the center of the CMZ, and for, respectively, $h = 2$ and 2.5 mm. The model curves of Figures 8 and 9 are plotted using the turbulent-flow equations (Eqs. 51 and 53). It appears that for these high rotation speeds the influence of the recirculation flow rate on the micromixing time becomes negligible. Thus, at the feed point situated at $d = 40.0$ mm from the center of the CMZ, when the rotating speed exceeds 40 s^{-1}, it is possible to change the reagent flow rates, and consequently, the residence time inside the CMZ without changing the micromixing time.

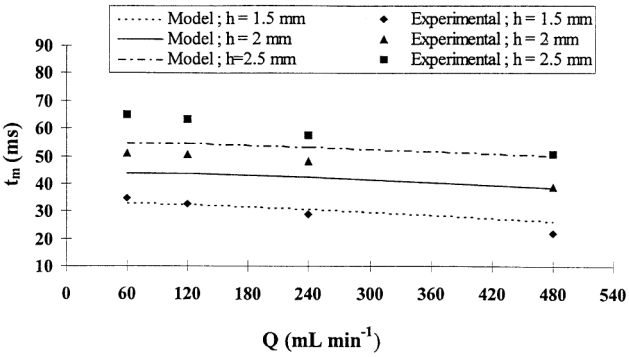

Figure 6. Measured and predicted micromixing times for various disk heights (for $N = 12$ s^{-1} and $r = 40.0$ mm).

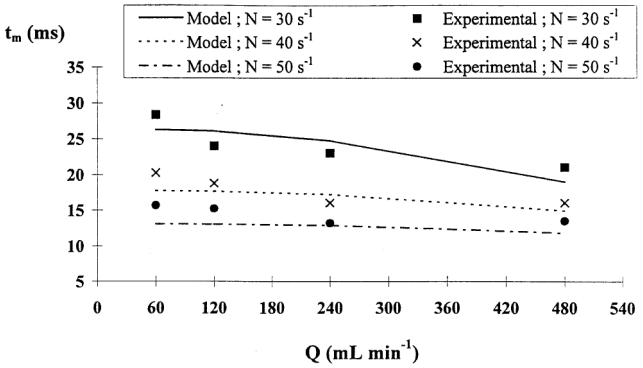

Figure 8. Measured and predicted micromixing times for various rotation speeds (for $r = 40.0$ mm and $h = 2.0$ mm).

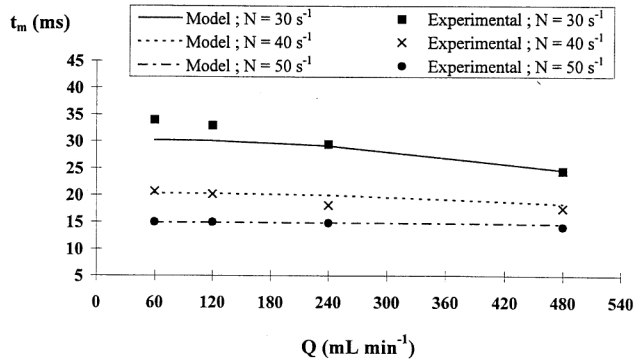

Figure 9. Measured and predicted micromixing times for various rotation speeds (for $r = 40.0$ mm and $h = 2.5$ mm).

Figures 10 and 11 refer to the experiments carried out at the feed point situated at $d = 17.5$ mm from the center of the CMZ, and for, respectively, $h = 1.5$ and 2 mm. The model curves of Figures 10 and 11 are plotted using the laminar-flow equations (Eqs. 51 and 52). It appears that for these operational conditions the recirculation flow rate has a strong influence on the micromixing time, except for a rotation speed of 50 s^{-1}, at which the recirculation flow rate seems to have almost no influence on the micromixing time.

Figure 12 shows agreement between the experimental results and Eqs. 51, 52, and 53. It is noteworthy that the experimental micromixing times at the injection point situated at 40.0 mm from the center are located between 12 and 58 ms, while those at the injection point situated at 17.5 mm from the center are located between 20 and 105 ms.

The sliding-surface mixing device of this study gives micromixing times varying from approximately 10 ms to approximately 100 ms. Thus, this new mixing device seems to be suitable for carrying out fast chemical reactions. Equations 51, 52, and 53 predict micromixing time values with an error that is generally smaller than 30%. These equations are obtained from hydrodynamic and dimensional analysis considerations, so they can be used for extrapolation. Micromixing time values smaller than 10 ms can be obtained by varying the diameter of the disk, the location of the injection point, and other operating parameters (rotation speed, height of the disk, flow rate).

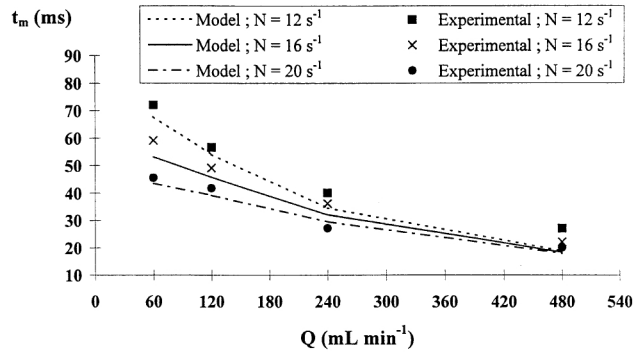

Figure 10. Measured and predicted micromixing times for various rotation speeds (for $r = 17.5$ mm and $h = 1.5$ mm).

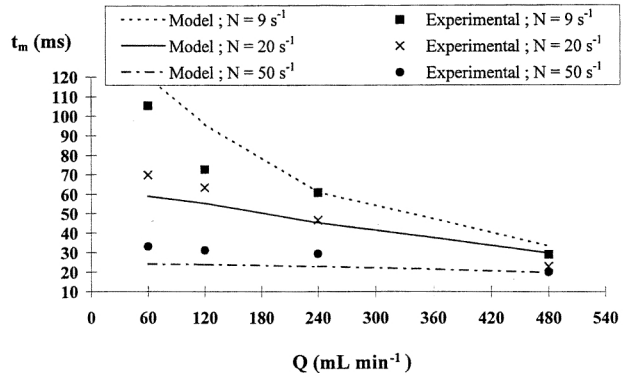

Figure 11. Measured and predicted micromixing times for various rotation speeds (for $r = 17.5$ mm and $h = 2.0$ mm).

Conclusions

In this article a new mixing device, called the sliding-surface mixing device, is studied. This reactor is characterized by a confined mixing zone (CMZ) in which very high shearing stresses are created in a very small volume so as to achieve effective micromixing of entering reagents.

The chemical system proposed by Villermaux and coworkers (1992) is successfully used for experimental determination of the micromixing time. The statistical treatment of the data shows that the chemical method used in this study gives micromixing time values with a relative error lower than 15%.

A model of micromixing inside the CMZ is developed taking all characteristics of the system into account. These characteristics are of two kinds: (1) process parameters, which are rotating speed and recirculation flow rate, and (2) geometric parameters, which are gap height and location of the injection feed tube.

Two flow regimes are identified thanks to the rotational Reynolds number: the laminar flow regime ($Re < 10^5$), and turbulent flow regime ($Re > 2 \cdot 10^5$). Two expressions that take these four parameters into account when predicting micromixing time are developed for laminar and turbulent flows. These expressions successfully predict the micromixing time and can be used for extrapolation purposes.

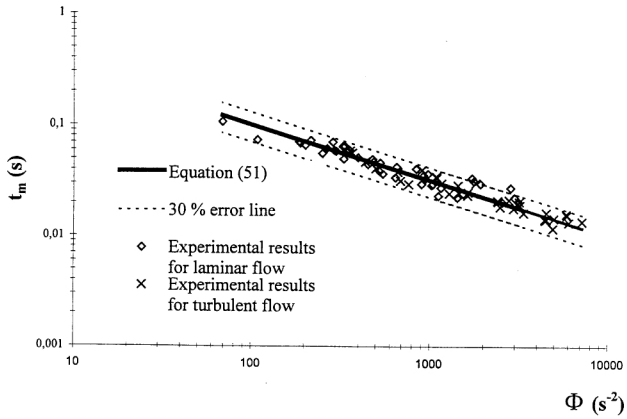

Figure 12. Measured vs. calculated micromixing times in the case of laminar and turbulent flows.

The sliding-surface mixing device used in this study gave micromixing time values that varied between approximately from 10 to 100 ms. Nevertheless, Eqs. 51, 52, and 53 allow the design of new devices and the determination of operating parameter values for attaining micromixing times lower than 10 ms.

Our study shows that the sliding-surface mixing device is a mixing apparatus that allows the micromixing time to be easily varied over a wide range by varying the rotation speed, the gap height between the disk and the bottom, the position of the lateral feed tubes, and the reagent flow rates. In addition, when the rotating speed exceeds 40 s^{-1}, at the feed point situated at $d = 40.0$ mm from the center of the CMZ, the influence of the reagent flow rates on the micromixing time becomes negligible. Hence, for high rotation speeds, it is possible to change the residence time inside the CMZ without changing the micromixing time. In addition, unlike jet mixers, for which high flow rates are compulsory in order to introduce high levels of power dissipation, the sliding-surface mixing device can be operated with low reagent flow rates without affecting the micromixing time. Finally, this device, which is easy to operate, can be successfully used for other industrial processes such as polymerization and formulation processes.

Acknowledgment

The authors are grateful for the financial support from the European Commission through BRITE-EURAM III Project, and to Miss M. Camps and Mr. B. Szikola for assistance in the experimental manipulations.

Notation

A_T^{aq}, B_T^{aq} = parameters of the model in the case of turbulent flow in Eq. 50, $m^{-3/2} \cdot s^{-19/4}$, $m^{-8/5} \cdot s^{-5}$
C_{Ao} = initial concentration of A in the tank, $mol \cdot L^{-1}$
C_{Bo} = concentration of B in the feed, $mol \cdot L^{-1}$
D = diffusivity, $m^2 \cdot s^{-1}$
E = incorporation (or engulfment) rate coefficient, s^{-1}
F = force, N
pH* = iodine dismutation pH
p = pressure, Pa
Sc = Schmidt number
t_r = chemical reaction time of reaction ii, s
ρ = density, $kg \cdot m^{-3}$
Φ = function depending on Reynolds number (see Eqs. 52 and 53), s^{-2}
ω = angular rotation speed, $rad \cdot s^{-1}$

Subscripts

1 = contribution of the spinning disk to the local energy dissipation
2 = contribution of the recirculation flow to the local energy dissipation

Literature Cited

Baldyga, J., and J. R. Bourne, "Comparison of the Engulfment and the Interaction-by-Exchange-with-the-Mean Micromixing Models," *Chem. Eng. J.*, **45**, 25 (1990).
Baldyga, J., and J. R. Bourne, "Interactions Between Mixing on Various Scales in Stirred Tank Reactors," *Chem. Eng. Sci.*, **47**, 1839 (1992).
Baldyga, J., J. R. Bourne, and Yang Yang, "Influence of Feed Pipe Diameter on Mesomixing in Stirred Tank Reactors," *Chem. Eng. Sci.*, **48**, 3383 (1993).
Baldyga, J., A. Rozen, and F. Mostert, "A Model of Laminar Micromixing with Application to Parallel Chemical Reactions," *Chem. Eng. J.*, **69**, 7 (1998).
Bolzern, O., and J. R. Bourne, "Rapid Chemical Reactions in a Centrifugal Pump," *Chem. Eng. Res. Des.*, **63**, 275 (1985).
Bourne, J. R., and J. Garcia-Rosas, "Rotor-Stator Mixers for Rapid Micromixing," *Chem. Eng. Res. Des.*, **64**, 11 (1986).
Bourne, J. R., F. Kozicki, U. Moergeli, and P. Rys, "Mixing and Fast Chemical Reaction: III. Model-Experiment Comparisons," *Chem. Eng. Sci.*, **36**(10), 1655 (1981).
Bourne, J. R., and M. Studer, "Fast Reactions in Rotor-Stator Mixers of Different Size," *Chem. Eng. Process*, **31**, 285 (1992).
Bourne, J. R., and S. A. Thoma, "Some Factors Determining the Critical Feed Time of a Semi-Batch Reactor," *Trans. Inst. Chem. Eng.*, **69**(A), 321 (July, 1991).
Bourne, J. R., and G. Tovstiga, "Micromixing and Fast Chemical Reactions in a Turbulent Tubular Reactor," *Chem. Eng. Res. Des.*, **66**, 26 (1988).
Deglon, D. A., C. T. O'Connor, and A. B. Pandit, "Efficacy of a Spinning Disk as a Bubble Break-Up Device," *Chem. Eng. Sci.*, **53**, 59 (1998).
Fournier, M. C., "Caractérisation de l'Efficacité de Micromélange par une Nouvelle Réaction Chimique Test," PhD Thesis, Institut National Polytechnique de Lorraine, Nancy, France (1994).
Fournier, M. C., L. Falk, and J. Villermaux, "A New Parallel Competing Reaction System for Assessing Micromixing Efficiency—Determination of Micromixing Time by a Simple Mixing Model," *Chem. Eng. Sci.*, **51**, 5187 (1996).
Franke, J., and A. Mersmann, "The Influence of the Operational Conditions on the Precipitation Process," *Chem. Eng. Sci.*, **50**, 1737 (1995).
Guichardon, P., "Caractérisation Chimique du Micromélange par la Réaction Iodure-Iodate: Application aux Milieux Visqueux et aux Suspensions Liquide-Solide," PhD Thesis, Institut National Polytechnique de Lorraine, Nancy, France (1996).
Incropera, F. P., and D. P. DeWitt, *Fundamentals of Heat and Mass Transfer*, 4th ed., Wiley, New York (1996).
Klein, J.-P., R. David, and J. Villermaux, "Interpretation of Experimental Liquid Phase Micromixing Phenomena in a Continuous Stirred Reactor with Short Residence Times," *Ind. Eng. Chem. Fundam.*, **19**, 373 (1980).
Li, K. T., and H. L. Toor, "Turbulent Reactive Mixing with a Series-Parallel Reaction: Effect of Mixing on Yield," *AIChE J.*, **32**, 1312 (1986).
Marcant, B., and R. David, "Experimental Evidence for and Prediction of Micromixing Effects in Precipitation," *AIChE J.*, **37**, 1698 (1991).
Palmer, D. A., and M. H. Lietzke, "The Equilibria and Kinetics of Iodine Hydrolysis," *Radiochim. Acta*, **31**, 37 (1982).
Plasari, E., R. David, and J. Villermaux, "Micromixing Phenomena in Continuous Stirred Reactors Using a Michaelis-Menten Reaction in the Liquid Phase," *Chemical Reaction Engineering-Houston*, ACS Symposium Series 65, Washington, DC, p. 125 (1978).
Pohorecki, R., and J. Baldyga, "The Effects of Micromixing and the Manner of Reactor Feeding on Precipitation in Stirred Tank Reactors," *Chem. Eng. Sci.*, **43**, 1949 (1988).
Schlichting, H., *Boundary Layer Theory*, 6th ed., McGraw-Hill, New York (1968).
Villermaux, J., "Micromixing Phenomena in Stirred Reactors," *Encyclopedia of Fluid Mechanics*, Gulf Pub., Houston, TX, p. 233 (1986).
Villermaux, J., "Micromixing and Chemical Reaction: Semi-Quantitative Criteria Based on Characteristic Time Constants," AIChE Meeting, Chicago (1990).
Villermaux, J., L. Falk, and M. C. Fournier, "Use of Parallel Competing Reactions to Characterize Micromixing Efficiency," *AIChE Symp. Ser.*, **286**(88), 6 (1992).
Villermaux, J., L. Falk, and M. C. Fournier, "Potential Use of a New Parallel Reaction System to Characterize Micromixing in Stirred Reactors," *AIChE Symp. Ser.*, **299**(90), 50 (1994).

Manuscript received Feb. 4, 1999, and revision received June 14, 1999.